Experimental Evidence of the Symmetry Breakdown in 4,8-Diethoxy-2,7-bis(benzo-1′,3′-dithiol-2′-ylidene)-1,3,5,7-tetrathia-*s*-indacene Compounds

K. Pokhodnia,[†] P. Cassoux,* J. Bonvoisin,[‡] A. Mlayah,[§] L. Brossard,[§] S. Frenzel,[||] and K. Müllen[||]

Institute of Semiconductors NASU, av. Nauki, 45, Kiev, Ukraine, LCC-CNRS, 205 Route de Narbonne, 31077 Toulouse Cedex, France, CEMES-CNRS, 29 Rue Jeanne-Marvig, 31055 Toulouse Cedex, France, Service National des Champs Magnétiques Pulsés du CNRS et Laboratoire de Physique des Solides, Complexe Scientifique de Rangueil, 31077 Toulouse Cedex, France, and Max Planck Institut für Polymerforschung, Postfach 3148, 55021 Mainz, Germany

Received: July 24, 1996; In Final Form: February 3, 1997[⊗]

The visible−near-IR absorption spectra of a bis(TTF) molecule, 4,8-diethoxy-2,7-bis(benzo-1′,3′-dithiol-2′-ylidene)-1,3,5,7-tetrathia-*s*-indacene (**1**), and of the corresponding monocationic species $\mathbf{1}^{\bullet+}$ generated by chemical or electrochemical oxidation are reported. IR and Raman studies of **1** and the derived $\mathbf{1}_x PF_6$ salt and ESR studies of $\mathbf{1}^{\bullet+}$ are described. The results of this experimental investigation are compared with those of semiempirical calculations performed using the PM3 or AM1 modeling and simulation programs, and of a normal coordinate analysis. This comparison affords additional evidence for a symmetry breakdown in radical cations based on such bis(TTF) systems. An asymmetrical spin density distribution in the $\mathbf{1}^{\bullet+}$ radical cation is also confirmed by ESR measurements.

I. Introduction

The design of molecules, in which long-distance electron transfer occurs between a donor site and an acceptor site though a conjugated bridging ligand, remains a challenge for molecular electronics.[1] The resulting "molecular wires" are key elements of molecule-based electronic devices such as switches.[2] Inorganic mixed-valence systems in which the donor and acceptor sites are transition metal ions in different oxidation states are the simplest model examples for studying such intramolecular electron transfer. As such, the prototypical Creutz−Taube complex, $[(NH_3)_5Ru^{II}(pyrazine)Ru^{III}(NH_3)_5]^{5+}$, has been extensively studied.[3] These are *intramolecular* mixed-valence systems in which the electronic interactions between the two redox sites are propagated within the molecule through the bridging group.

Intramolecular mixed-valence systems in which the two redox sites are purely organic are not very common.[4] Several "bis(TTF)" (4,8-diethoxy-2,7-bis(benzo-1′,3′-dithiol-2′-ylidene)-1,3,5,7-tetrathia-*s*-indacene) systems, i.e., compounds containing two TTF moieties connected by aromatic bridging groups, have been reported.[5,6] Electrochemical studies of these bis(TTF) compounds show four successive, reversible one-electron oxidations, consistent with the sequential formation of the mono-, di-, tri-, and tetracationic species.[5−8]

In a previous study,[7,8] some of us have observed in the near-IR spectra of several bis(TTF)$^{\bullet+}$ radical cations a rather intense and broad band that has been identified as an "intervalence transition" characteristic of intramolecular mixed-valence species.[3] This interpretation was nicely corroborated by theoretical calculations at semiempirical and *ab initio* levels.[8] The main result of these calculations was the observation of a symmetry breakdown when going from the neutral to the monocationic form of bis(TTF). This symmetry breakdown is readily displayed when comparing the optimized central C═C bond distance in the $S_2C{=}CS_2$ fragment of each TTF subunit of neutral bis(TTF) compounds with their corresponding bis(TTF)$^{\bullet+}$ radical cations. In neutral bis(TTF) this distance is identical in both TTF subunits (1.351 Å) and almost identical with the corresponding distance in neutral TTF (1.349 Å),[9] while in bis(TTF)$^{\bullet+}$ the central C═C bond distance of *only one* TTF subunit increases to 1.427 Å, which is closer to the typical C═C bond distance in a TTF$^{\bullet+}$ salt such as $(TTF)ClO_4$ (1.404 Å).[10] The reduction of symmetry of the bis(TTF) molecule upon oxidation should cause significant changes of its vibrational modes that could be confirmed by IR and/or Raman studies.

In this paper, we report on the visible−near-IR absorption spectra of a bis(TTF) molecule 4,8-diethoxy-2,7-bis(benzo-1′,3′-dithiol-2′-ylidene)-1,3,5,7-tetrathia-*s*-indacene (**1**) (Figure 1) and the derived radical cation $\mathbf{1}^{\bullet+}$, on IR and Raman studies of **1** and the derived $\mathbf{1}_x PF_6$ salt, and on ESR studies of $\mathbf{1}^{\bullet+}$. The results of this investigation, together with those of new semiempirical calculations, afford additional evidence for a symmetry breakdown in radical cations based on such bis(TTF) systems.

II. Experimental Section

(a) Synthesis and Electrochemical Studies. Bis(fulvalene), 4,8-diethoxy-2,7-bis(benzo-1′,3′-dithiol-2′-ylidene)-1,3,5,7-tetrathia-*s*-indacene (**1**), has been prepared as previously described.[11] Electrochemical studies were carried out with techniques and apparatus similar to those used in a previous investigation of analogous bis(TTF) systems.[8] The values of the half-wave potentials for all four reversible one-electron transfer steps are comparable with those previously reported.[11] The corresponding radical cation $\mathbf{1}^{\bullet+}$ has been generated both electrochemically and by chemical oxidation. The electrolysis of solutions of **1** (0.1 M to 0.3×10^{-3} M) in degassed anhydrous

* To whom correspondence should be addressed. Address: Equipe Précurseurs Moléculaires et Matériaux, LCC-CNRS, France. E-mail: cassoux@lcc-toulouse.fr.

[†] Institute of Semiconductors NASU. Present address: Institute Joseph Stefan, University of Ljubljana, Jamova, 39, Ljubljana 1001, Slovenia.

[‡] Groupe Electronique Moléculaire, CEMES-CNRS.

[§] Service National des Champs Magnétiques Pulsés du CNRS et Laboratoire de Physique des Solides.

[||] Max Planck Institut für Polymerforschung.

[⊗] Abstract published in *Advance ACS Abstracts,* April 1, 1997.

S1089-5647(96)02246-8 CCC: $14.00

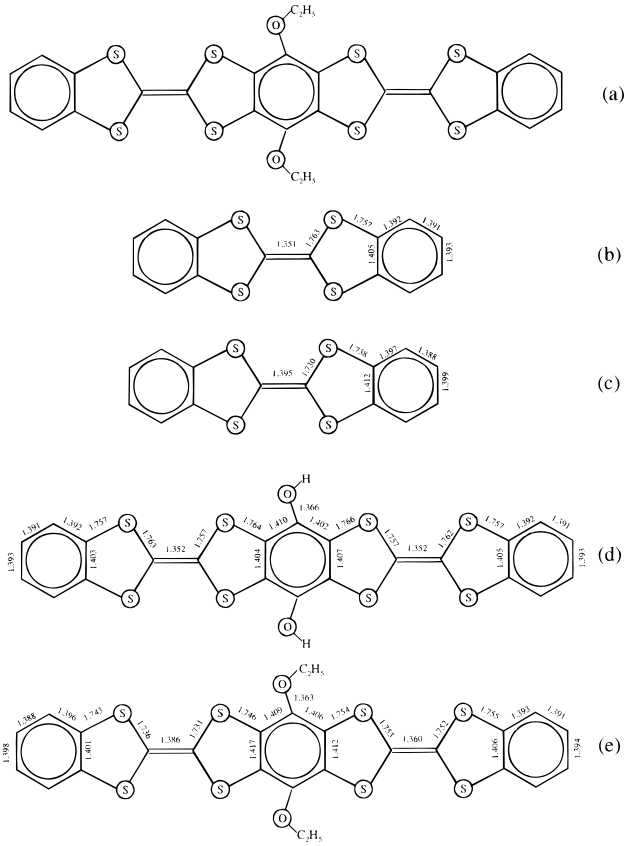

Figure 1. 4,8-Diethoxy-2,7-bis(benzo-1′,3′-dithiol-2′-ylidene)-1,3,5,7-tetrathia-*s*-indacene molecule (**1**) (a), calculated geometries of DBTTF (b), DBTTF$^+$ (c), and the model systems **I** (d) and **I**$^{\bullet+}$ (e).

CH_2Cl_2 containing (n-Bu_4N)PF_6 (0.1 M) was carried out in an airtight three-electrode cell connected to a vacuum/argon line. Coulometric experiments were performed at room temperature on a platinum electrode with a large surface area (ca. 15 cm^2) at a potential slightly more positive than the first half-wave oxidation potential. After one electron for the first oxidation step was counted, the generated **1**$^{\bullet+}$ radical cation solution was syringed for optical and ESR studies. During electrolysis, a small amount of a solid, presumably a bis(TTF) radical cation salt, $\mathbf{1}_x PF_6$, precipitates from the solution. This precipitate was separated by centrifugation, washed in CH_2Cl_2, and dried under vacuum. Observation of the precipitate with an optical microscope shows that it consists of needle-like microcrystals. Solutions of the radical cation **1**$^{\bullet+}$ were also obtained by direct oxidation of the neutral molecule with a 1:1:10 mixture of $CF_3COOH/(CF_3CO)_2O/CH_2Cl_2$ for 10 h. In this case, no precipitation of any radical cation salt was observed.

(b) Optical Spectroscopy. Absorption spectra of **1** and **1**$^{\bullet+}$ in solution and $\mathbf{1}_x PF_6$ in KBr pellets were recorded with a Shimadzu UV 101 PC spectrometer in the visible−near-IR spectral range and with a Perkin-Elmer (Model PE 1725) spectrometer in the IR range 400−4000 cm^{-1}. The Raman spectra of polycrystalline samples were recorded with a DILOR XY spectrometer, and the samples were excited with the 413.1 and 488.0 nm lines of a mixed Kr−Ar gas laser.

(c) ESR Spectroscopy. The ESR spectra of CH_2Cl_2 solutions of the radical cation **1**$^{\bullet+}$ generated by both electrochemical and chemical methods were recorded with a Bruker ESP 300E instrument equipped with a Bruker ER 035M gauss meter and an EIP 548 microwave frequency counter operating at the X-band in the temperature range 100−300 K.

(d) Calculations. Full geometry optimization without symmetry restraint was performed for dibenzotetrathiafulvalene DBTTF, DBTTF$^{\bullet+}$, and the model bis(TTF) compound **I** and its radical cation **I**$^{\bullet+}$ (Figure 1) at the semiempirical PM3 and AM1 levels with the restricted Hartree−Fock (RHF) basis (for **I** and **I**$^{\bullet+}$) and restricted open Hartree−Fock (ROHF) basis (for methyl-substituted **I**$^{\bullet+}$) using the HyperChem or MOPAC93 package.[12] In a previous similar study, such semiempirical methods were proved to yield satisfactory results for geometry optimization of similar bis(TTF) systems compared to ab initio methods.[8] In the case of the open-shell radical cations, the half-electron method was used. Configuration interaction (CI) calculations were performed for obtaining the spectra of electron excitations in the visible and UV ranges. From the reference (ground-state) configuration, excited configurations were generated by promoting electrons from the three occupied orbitals closest to the HOMO level into three unoccupied (virtual) orbitals closest to the LUMO (only singly excited configurations were involved in our CI calculations). Since HyperChem allows the excited-state oscillator strength to be computed, only spectroscopically active electron transitions were taken into consideration. The vibration analysis of all listed compounds was performed. The Hessian matrix was evaluated by finite difference of analytical gradients and diagonalized to determine normal modes and harmonic frequencies.

III. Results and Discussion

The results of the geometry optimization for DBTTF, DBTTF$^{\bullet+}$, and the model systems **I** and **I**$^{\bullet+}$ are shown in Figure 1. Similar bond length values of the C═C and S−C bonds in the $S_2C{=}CS_2$ fragments have been found for DBTTF and **I**. It is known that ionization causes a significant elongation of the central C═C bond (from 1.349 to 1.41 Å) as well as a shortening of the C−S bonds in the $S_2C{=}CS_2$ fragment of TTF due to a different contribution of these bonds (bonding and antibonding, respectively) to the HOMO level.[13] The calculated geometry changes in DBTTF upon the oxidation (the central C═C bond increases from 1.351 to 1.395 Å) are consistent with these experimental results.

As previously observed when comparing TTF$^+$ and similar bis(TTF)$^+$ radical cations,[8] a dramatic difference was found between DBTTF$^+$ and **I**$^{\bullet+}$; although DBTTF and **I** belong to the D_{2h} point group, a symmetry breakdown occurred for **I**$^{\bullet+}$, leading to a C_{2v} structure. This symmetry breakdown originates from a significant elongation of the central C═C bond and a shortening of the C−S bonds in the $S_2C{=}CS_2$ fragment of *only one* TTF subunit of **I**$^{\bullet+}$ (see parts d and e of Figure 1), while the lengths of the central C═C bond and the CS bonds in the $S_2C{=}CS_2$ fragment of *the other* TTF subunit remain close to the values calculated for neutral **I**. It should be noted that substituting OMe groups for OH groups on the bridge results in a more pronounced symmetry breakdown (1.352 Å for both central C═C bonds in the neutral molecule compared to 1.340 and 1.414 Å in the radical cation), which seems to indicate that the nature of the substituents on the bridge may affect the symmetry of a bis(TTF)$^{\bullet+}$ radical cation.

These remarkable bond length modifications were also reflected in the calculated net charge partitions (i.e., the sum of the net charges carried by the atoms of the $S_2C{=}CS_2$ fragments) and in the spin density distribution (Figure 2). The net charge partitions (CP) on only one $S_2C{=}CS_2$ fragment of **I**$^{\bullet+}$ is equal to 1.079 (a value that is close to 1.154 calculated for DBTTF$^{\bullet+}$), while on the other $S_2C{=}CS_2$ fragment, CP is equal to 0.661 (for neutral DBTTF, CP is equal to 0.428). The contour plot of the spin density distribution also shows that the spin density is localized mainly on only one $S_2C{=}CS_2$ fragment of **I**$^{\bullet+}$.

Possible spectroscopically active electronic transitions in the investigated systems were subsequently calculated using con-

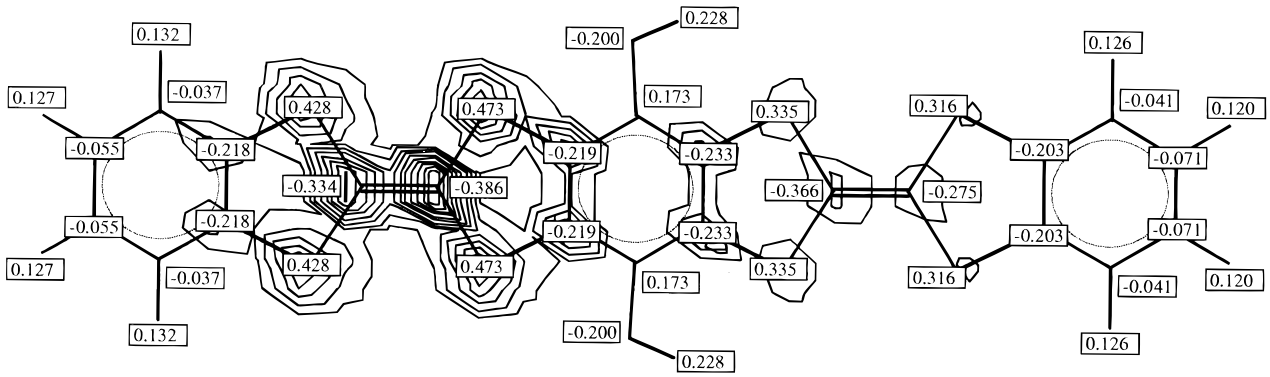

Figure 2. Net charge partitions and spin density distribution in model system $\mathbf{I}^{\bullet+}$.

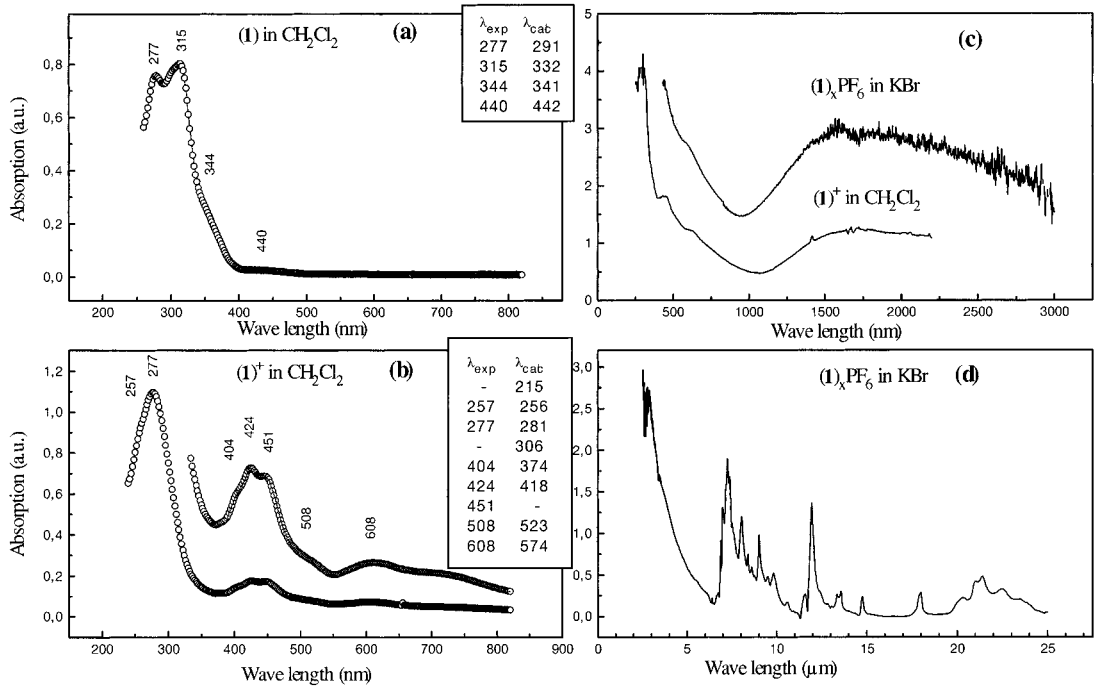

Figure 3. Absorption spectra of **1** (a) and $\mathbf{1}^{\bullet+}$ (b) in CH_2Cl_2 and CH_3CN in the visible region, of $\mathbf{1}^{\bullet+}$ in CH_2Cl_2 and $\mathbf{1}_x PF_6$ in KBr in the near-IR region (c), and of $\mathbf{1}_x PF_6$ in KBr in the infrared spectral range (d). The experimental and calculated band positions are presented in the inserted tables.

figuration interaction, and their energies were compared with the results of visible−near-IR studies. The absorption spectra of **1** and $\mathbf{1}^{\bullet+}$ in the visible region are shown in Figure 3. In the spectrum of the neutral molecule, two intense lines at 277 and 315 nm were observed. These data are in agrement with the results of Räder et al.,[11] who assigned these lines to the lowest energy $\pi-\pi^*$ transitions. The small difference in the energies of these transitions in DBTTF and **1** was considered an indication of a slight structural variation of the benzo-TTF fragments after being linked together in **1** via a π-conjugated ring.[11] This assumption is corroborated by our semiempirical calculations, which indicate only slight changes of the corresponding bond lengths. It should be noted that considerably less intense features, namely, a shoulder at 344 nm and a line at 440 nm, can also be observed in the measured spectrum of **1**. Our CI calculations also predict two additional transitions at 341 and 442 nm.

An intense absorption resulting from a $\pi-\pi^*$ transition is also observed at 277 nm in the spectrum of the $\mathbf{1}^{\bullet+}$ radical cation in CH_2Cl_2, but five additional, less intense lines at 404, 424, 451, 508, and 608 nm are clearly seen as well. Since these lines are not observed in the spectrum of the neutral molecule **1**, they are probably connected with electron transitions to the partially filled HOMO. Our CI calculations of UV−visible spectra of model systems **I** and $\mathbf{I}^{\bullet+}$ confirm this assumption and are in good qualitative agreement with the experimental data (see tables in parts a and b of Figure 3).

The most interesting feature in the absorption spectrum of $\mathbf{1}^{\bullet+}$ is a broad (full width at half-maximum fwhm = 5000 ± 500 cm^{-1}) and moderately intense band ($\epsilon = (10 \pm 3) \times 10^3$ M^{-1} cm^{-1}) centered around 1600−1700 nm (Figure 3c). Since the intensity of this band in the solution spectrum follows the Beer's law over a concentration range $10^{-4}-10^{-5}$ M, its appearance cannot be explained by any aggregated form of radical cations in solution but certainly reveals the peculiarities of the radical cation's electronic structure. A low-energy band at 1040 nm associated with an electron transition from the double occupied orbital nearest the HOMO to the single occupied HOMO level was also found in the calculated spectrum of $\mathbf{I}^{\bullet+}$. Since the π-electron density associated with these orbitals is inversely distributed, this band may be assigned as a charge-transfer transition, known as "intervalence transition",[3] between two slightly coupled TTF subunits. Such an assignment was also previously suggested for a series of analogous bis-$(TTF)^{\bullet+}$ cation radicals[8] and is indicative of a mixed-valence state in bis$(TTF)^{\bullet+}$ radical cations, which is confirmed by the calculations. The shape and the intensity of this band indicate

that $\mathbf{1}^{\bullet+}$ is a class II mixed-valence compound, i.e., it possesses a localized electronic structure.[14]

It should be noted that the same band is observed at 1600−1700 nm in the spectrum of polycrystalline samples of $\mathbf{1}_x PF_6$ in KBr pellets (parts c and d of Figure 3). This band is somewhat broader than that observed in the spectrum of $\mathbf{1}^{\bullet+}$ in solution and may be a superposition of two bands originating from intra- and intermolecular electron transitions. Such an intermolecular electron transition was observed in the concentrated solution of dications of similar bis(TTF) compounds at 950 nm.[8] Its higher energy is apparently connected with the stronger on-site Coulomb interaction. The possibility of intermolecular charge transfer in $\mathbf{1}_x PF_6$ may be reflected in preliminary single-crystal conductivity measurements, which show rather high values, $\sigma = 10^{-2}$ S cm^{-1} at room temperature along the needle.

The idea of an asymmetrical distribution of the unpaired electron density in bis(TTF)$^{\bullet+}$ radical cations should be confirmed by Raman and infrared studies. However, before we start the discussion of the results of such studies that we have carried out for **1** and $\mathbf{1}_x PF_6$, it should be recalled that the interpretation of the Raman and IR spectra of radical cation salts of TTF and its derivatives is usually based on the concept of "ionization shift" of the frequencies of the C═C and C−S stretching modes of the $S_2C{=}CS_2$ fragment with respect to their values in the neutral molecule.[15,16] In the vibration spectra of the radical cation salts, the elongation of the C═C bond results in a red (negative) shift of the C═C stretching modes, and the shortening of the C−S bonds causes a blue (positive) shift of the C−S stretching modes.

There are two A_g modes involving mainly the C═C stretching in TTF-based molecules with D_{2h} symmetry. They are observed in the Raman spectra of these compounds in the region 1500−1550 cm^{-1} and correspond to the out-of-phase and in-phase stretching of the central and ring C═C bonds. In the spectra of TTF-based radical cations, these modes show a negative ionization shift of about 50 cm^{-1} for the first mode and 100−120 cm^{-1} for the second one.[15−17] According to our normal coordinate analysis performed at the semiempirical level for DBTTF and its radical cation, the corresponding negative shifts calculated for these modes, 39 and 151 cm^{-1}, respectively, are in a good qualitative agreement with the experimental data. The calculated frequencies are only 10% higher than their experimental values[18] (the overestimation of stretching vibration frequencies is a common disadvantage of all NDO semiempirical methods, but PM3 shows the closest correspondence to the experimental values[19]).

Since the bis(TTF) molecule (**1**) has 156 normal modes, the complete assignment of them would be a very difficult task. We therefore concentrated our attention on the totally symmetrical C═C bonds stretching modes, since their position in the spectrum is very sensitive to the peculiarities of the charge distribution in TTF-based molecules. The normal coordinate analysis performed for model system **I** (assuming a D_{2h} symmetry) shows that three A_g modes containing C═C bond stretching should exist in the Raman spectra: (a) the in-phase stretching motion of the C═C bonds in the peripheric benzene rings (PBR) and the central benzene ring (CBR), together with a contraction of the C═C bonds in the $S_2C{=}CS_2$ fragments; (b) the in-phase stretching of the C═C bonds in PBR and $S_2C{=}CS_2$ fragments, together with a contraction of the C═C bonds in CBR; (c) the in-phase stretching of the C═C bonds in all fragments mentioned above. The calculated frequencies of these modes are located in the same region as for the modes mentioned above for DBTTF.[18]

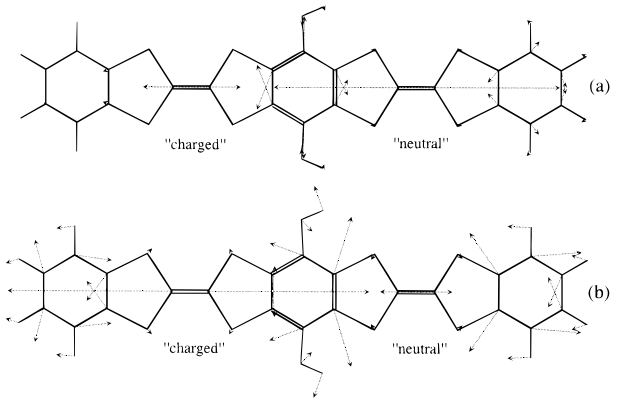

Figure 4. Class 1 (a) and class 2 (b) stretching modes of the $\mathbf{I}^{\bullet+}$ model system (the atomic displacements are increased about 500 times). Designations "charged" and "neutral" represent the asymmetry of the charge distribution.

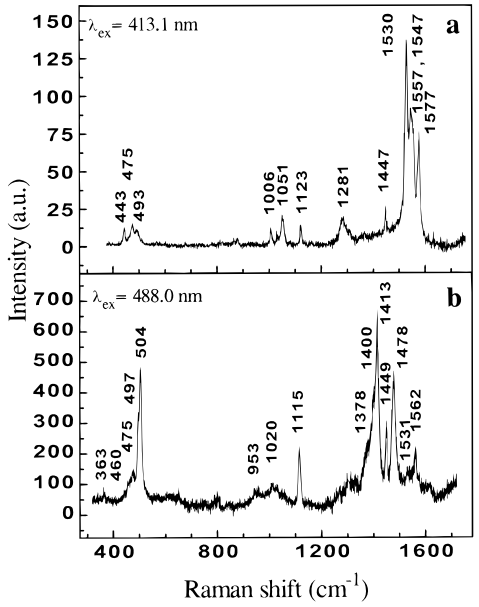

Figure 5. Raman spectra of **1** (a) and $\mathbf{1}_x PF_6$ (b) in KBr.

The remarkable changes in the vibration spectra of $\mathbf{1}_x PF_6$ have been predicted by the normal coordinate analysis and the valence force field calculations carried out for model system $\mathbf{I}^{\bullet+}$. Owing to the symmetry breakdown, the molecule has lost the center of inversion and its symmetry point group is reduced to C_{2v}. For this point group, the totally symmetrical A_1 modes can be qualitatively divided into two classes: (1) the modes corresponding to the in-phase stretching of the C═C bonds in PBR, CBR, and $S_2C{=}CS_2$ fragments (former A_g modes in the neutral molecule (Figure 4)a); (2) the modes corresponding to the out-of-phase stretching of the C═C bonds in the above-mentioned fragments (former B_{1u} modes in the neutral molecule (Figure 4b)).

The ionization shifts of the class 1 modes with respect to the corresponding modes in the neutral molecule are predicted to be about 10−30 cm^{-1}. They are mainly Raman-active, while the class 2 modes should show a significant ionization shift that may reach values up to 150−200 cm^{-1}. These modes should have high intensities both in Raman and infrared spectra.

After this qualitative insight into the nature and energies of vibration modes in bis(TTF) compounds, we can compare the predictions of our semiempirical calculations with the experimental data (see Figures 5 and 6). According to our analysis, the intense modes at 1577, 1547, and 1530 cm^{-1} observed in the Raman spectrum of **1** (Figure 5a) apparently are C═C bond-

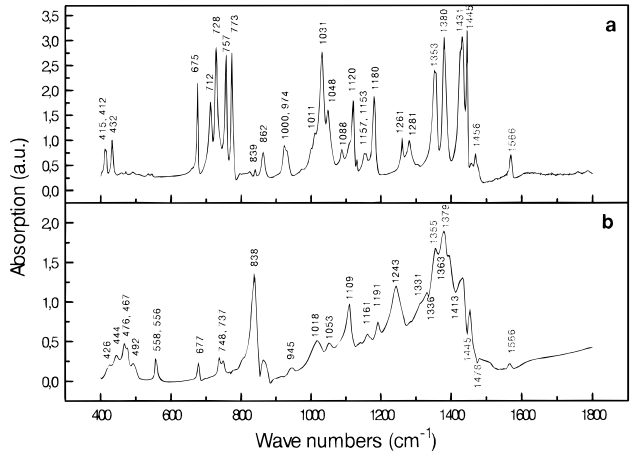

Figure 6. Infrared absorption spectra of **1** (a) and $\mathbf{1}_x PF_6$ (b) in KBr.

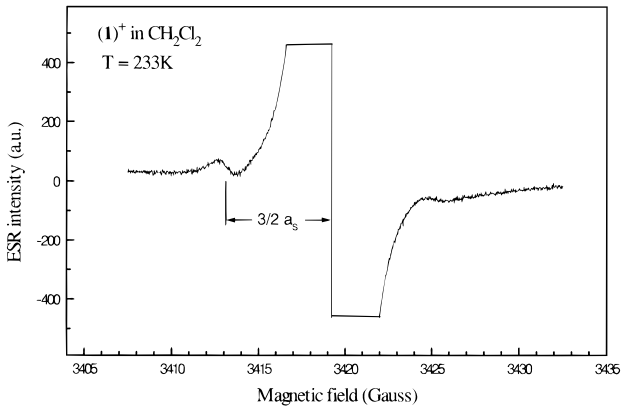

Figure 7. ESR spectrum of $\mathbf{1}^{\bullet+}$ in CH_2Cl_2 (T = 233 K).

stretching A_g modes of types a, b, and c. The poorly resolved shoulder at 1557 cm^{-1} probably corresponds to a B_{3g} mode of the inverse symmetrical stretching of the C═C bonds in CBR, also expected in this region. The corresponding infrared-active B_{1u} and B_{2u} modes should have, according to our calculations, very weak intensities except for the B_{1u} mode of the out-of-phase C═C bond stretching in PBR. Indeed, the only band that would correspond to this mode is observed at 1566 cm^{-1} in the infrared spectrum of the neutral molecule **1** (Figure 6a).

The region 400−500 cm^{-1} is characteristic of the C−S stretching vibrations of TTF and its derivatives. Thus, the bands at 443, 475, and 493 cm^{-1} in the Raman spectrum of **1** (Figure 5a) can be assigned to the A_g stretching vibrations of these bonds in the S_2C═CS_2 fragments. The corresponding antisymmetrical B_{1u} modes can be found in the infrared spectrum of **1** at 415 and 432 cm^{-1} (Figure 6a).

In the region of the C═C bonds stretching vibrations in the Raman spectrum of $\mathbf{1}_x PF_6$ (Figure 5b), two weak bands at 1531 and 1562 cm^{-1} are observed at nearly the same position as in the Raman spectrum of the neutral molecule **1**. Two very intense bands at 1478 and 1413 cm^{-1} and two shoulders at 1400 cm^{-1} and 1378 cm^{-1} are shifted by 100−200 cm^{-1} to the lower frequencies. This fits our model surprisingly well, and the first two unshifted bands can be assigned to the A_1 modes of class 1, while the strongly shifted modes can be assigned to A_1 modes of class 2.

The modes of class 1 should be mainly Raman active, and indeed, only one very weak band at 1566 cm^{-1} is observed in the 1500−1600 cm^{-1} region of the infrared spectrum of $\mathbf{1}_x PF_6$ (Figure 6b). On the other hand, the class 2 modes should be very intense in the infrared absorption. Unfortunately, the infrared spectrum of $\mathbf{1}_x PF_6$ in the region 1300−1450 cm^{-1} is not very clear. It consists of a broad envelope with several peaks and troughs as a fine structure. This is a typical shape for the infrared absorption spectrum in this region for TTF-based low-dimensional organic conductors, which has been associated with the electron−molecular vibrations coupling (EMVC) effect.[20,21] The mechanism of this effect can be described as an electron oscillation between the adjacent molecules with overlapping partially occupied MO (dimers) induced by the molecular vibrations. In such compounds, the totally symmetrical C═C and C−S bonds stretching modes have the highest EMVC constants.[22,23] In the presence of EMVC these normally infrared-inactive A_g modes become infrared-active for the light polarized in the direction of the dimer axis. Such an effect can be detected in the intense and broad so-called vibronic bands observed in the infrared spectrum of $\mathbf{1}_x PF_6$, which are shifted to frequencies lower than those arising from the parent A_g modes. In our case, it appears rather difficult to suggest whether in $\mathbf{1}_x PF_6$ the electron density oscillates between two TTF units within one $\mathbf{1}^{\bullet+}$ radical cation or between adjacent $\mathbf{1}^{\bullet+}$ radical cations, since both types of intra- or intermolecular electron transitions are possible in the investigated salt. Nonetheless, in the absence of additional polarization measurements, it may be assumed that the class 1 totally symmetrical C═C and C−S stretching modes can couple either with only one or with both electron relaxations and that the broad envelopes at 450 and 1400 cm^{-1} in the infrared spectrum of $\mathbf{1}_x PF_6$ are the manifestation of this EMVC effect.

In this case, class 2 A_1 modes may be antiresonances whose minima correspond to the vibrational feature frequencies. The minima at 1413 and 1478 cm^{-1} support this hypothesis. Some of the fine structure peaks may originate from intense CH_2 and CH_3 bending modes also expected in this region. For instance, the peak at 1447 cm^{-1} in the Raman spectrum of **1**, which is also observed at 1445 cm^{-1} in the IR spectrum, can be assigned to such bending modes. This peak remains practically unshifted in the Raman spectrum of $\mathbf{1}^{\bullet+}$ and reveals itself as a sharp antiresonance at 1445 cm^{-1} in the IR spectrum of this compound.

We have not overlooked the fact that in the $\mathbf{1}_x PF_6$ salt, which is not yet fully characterized, the actual charge of the radical cation is not known. Thus, conclusions drawn from the Raman and IR studies of this salt cannot be directly extended to the $\mathbf{1}^{\bullet+}$ monocationic species generated in solution by oxidation. Nonetheless, the present normal coordinate analysis and the valence force field calculations strongly suggest the localization of an excess charge in one of the TTF subunits of the $\mathbf{1}_x PF_6$ radical cation salt. This is consistent with the symmetry breakdown inferred from theoretical calculations carried out for the **I** and $\mathbf{I}^{\bullet+}$ model systems and with the observation of an intervalence transition in the near-IR spectra of $\mathbf{1}^{\bullet+}$ and $\mathbf{1}_x PF_6$.

An additional confirmation of this symmetry breakdown in $\mathbf{1}^{\bullet+}$ is afforded by ESR experiments. Since the hyperfine constant a_x is roughly proportional to the electron spin density on the atom with a nonzero nuclear magnetic moment (^{33}S, ^{13}C, or ^{1}H in our case), its value should be significantly different for symmetrical and asymmetrical spin density distributions. For comparison, hyperfine parameters and g-factors for radical cations of TTF and a large set of its derivatives can be used.[24]

The ESR spectrum of CH_2Cl_2 solutions of $\mathbf{1}^{\bullet+}$ generated by both electrochemical and chemical methods consists of a single line (g = 2.0075, ΔH_{pp} = 0.2 mT) at room temperature (Figure 7). By varying the concentration and the temperature, we succeeded in decreasing ΔH_{pp} to 0.13 mT, but this value still remains an order of magnitude higher than that for TTF[24] presumably because of unresolved proton hyperfine structures.

Therefore, one can expect that only the ^{33}S hyperfine satellite can be resolved in the ESR spectrum, since the constant a_x for this nucleus is near 0.4 mT.

Indeed, when the gain is increased, a hyperfine satellite line, with an intensity of less than 1% of the main line and centered at 0.59 mT from the main line, is observed at the low-frequency side. A less intense satellite is observed on the high-field side as well. A similar, pronounced hyperfine anisotropy was earlier reported for TTF and its derivatives, especially for the ^{33}S isotope.[24] Assuming that the observed satellite is two of the four lines resulting from the hyperfine interaction between the unpaired electron and the ^{33}S isotope located in one of the four S-sites, one can calculate the corresponding hyperfine constant as $a_x = 0.4$ mT. This value is only about 5% lower than the ^{33}S hyperfine constant previously obtained for $DBTTF^{\bullet+}$,[24] which implies that the unpaired electron is localized mainly on only one of the $S_2C{=}CS_2$ fragments of the investigated $\mathbf{1}^{\bullet+}$ radical cation. The slightly smaller value for the ^{33}S hyperfine constant for $\mathbf{1}^{\bullet+}$ may be connected with the localization of some weak spin density on the opposite $S_2C{=}CS_2$ fragment (see Figure 2).

The solid-state ESR spectrum of the $\mathbf{1}_x PF_6$ salt consists of a broad asymmetric line with $\Delta H_{pp} \approx 1$ mT. Thus, no ^{33}S hyperfine satellite can be expected to be resolved. The asymmetry of the ESR line reflects the *g*-factor anisotropy that is typical for radical cation salts of TTF-like compounds.

In summary, the performed semiempirical calculations of bis(TTF) model systems **I** and $\mathbf{I}^{\bullet+}$ confirm the unexpected asymmetrical localization effect reported earlier for similar bis(TTF)$^+$ systems.[8] The observation of an intervalence transition in the near-IR spectra of $\mathbf{1}^{\bullet+}$ and $\mathbf{1}_x PF_6$ is in agreement with this symmetry breakdown hypothesis. The normal coordinate analysis and the calculation of the valence force field matrix carried out for model systems **I** and $\mathbf{I}^{\bullet+}$ allow us to predict the remarkable changes in the Raman and IR spectra observed when going from **1** to $\mathbf{1}_x PF_6$. An asymmetrical spin density distribution is also confirmed by ESR measurements on the $\mathbf{1}^{\bullet+}$ radical cation. Thus, the oxidation-induced symmetry breakdown in the investigated bis(TTF) system is experimentally validated.

Acknowledgment. The technical assistance for electrochemical, IR, and ESR studies from D. de Montauzon, C. David, and A. Mari is gratefully acknowledged. This work was supported in part by the University of Toulouse-Ukrainian Academy of Sciences Twinning Program (K.P.).

References and Notes

(1) Tanigaki, K. *Polymeric Materials for Microelectronic Applications*; ACS Symposium Series 579; American Chemical Society: Washington, DC, 1994; p 343.

(2) (a) *Molecular Electronic Devices*; Carter, F. L., Ed.; Marcel Dekker: New York, 1982. (b) *Molecular Electronic Devices II*; Carter, F. L., Ed.; Marcel Dekker: New York, 1987. (c) Woitellier, S.; Launay, J.-P.; Spangler, C. W. *Inorg. Chem.* **1989**, *28*, 758 .

(3) (a) Creutz, C. *J. Am. Chem. Soc.* **1969**, *91*, 3988. Creutz, C. *Prog. Inorg. Chem.* **1983**, *30*, 1. (b) Hush, N. S. *Coord. Chem. Rev.* **1985**, *64*, 135. (c) *Mixed Valency Systems: Applications in Chemistry, Physics and Biology*; Prassides, K., Ed.; NATO ASI Series; Kluwer Academic Publishers: Dordrecht, 1991.

(4) (a) Schroeder, A. H.; Mazur, S. *J. Am. Chem. Soc.* **1978**, *100*, 7339. (b) Utamapanya, S.; Rajca, A. J. *J. Am. Chem. Soc.* **1978**, *113*, 9242. (c) Nelsen, S. F.; Adamus, J.; Wolff, J. J. *J. Am. Chem. Soc.* **1994**, *116*, 7339. (d) Miller, L. L.; Liberko, C. A. *Chem. Mater.* **1994**, *2*, 339. (e) Bonvoisin, J.; Launay, J.-P.; Rovira, C.; Veciana, J. *Angew. Chem., Int. Ed. Engl.* **1994,** *33*, 2106. (f) Bonvoisin, J.; Launay, J.-P.; Van der Auweraer, M.; de Schryver, F. C. *J. Phys. Chem.* **1994**, *98*, 5052.

(5) Scherer, U.; Shen, Y.-J.; Adam, M.; Bietsch, W.; von Schütz, J. U.; Müllen, K. *Adv. Mater.* **1993**, *5*, 109.

(6) Lahlil, K.; Moradpour, A.; Merienne, C.; Bowlas, C. *J. Org. Chem.* **1994**, *59*, 8030.

(7) Cassoux, P.; Bowlas, C. J.; Lahlil, K.; Moradpour, A.; Bonvoisin, J.; Launay, J.-P. *Acta Phys. Pol. A* **1995**, *87*, 743.

(8) Lahlil, K.; Moradpour, A.; Bowlas, C. J.; Menou, F.; Cassoux, P.; Bonvoisin, J.; Launay, J.-P.; Dive, G.; Dehareng, D. *J. Am. Chem. Soc.* **1995**, *117*, 9995.

(9) Cooper, W. F.; Kenny, N. C.; Edmonds, J. W.; Nagel, A.; Wudl, F.; Coppens, P. *J. Chem. Soc., Chem. Commun.* **1971**, 889.

(10) Yakushi, K.; Nishimura, S.; Sugano, T.; Kuroda, H. *Acta Crystallogr. B* **1980**, *36*, 358.

(11) Räder, H.-J.; Scherer, U.; Müllen, P. K. *Synth. Met.* **1989**, *32*, 15.

(12) Dewar, M. J. S.; Yuan, Y. C. MOPAC 93.00. *Inorg. Chem.* **1990**, *29*, 3881. PM3 is a reparametrization of the AM1 method. See, for example, the following. Dewar, M. J. S.; Zoebisch, E. G.; Healy, E. F.; Steward, J. S. *J. Am. Chem. Soc.* **1985**, *107*, 3902.

(13) Williams, R.; Lowe Ma, C.; Samson, S.; Khana, S. K.; Samoano, R. B. *J. Chem. Phys.* **1980**, *72*, 3761.

(14) Robin, M. B.; Day, P. *Adv. Inorg. Radiochem.* **1967**, *10*, 247.

(15) Bozio, R.; Zanon, I.; Girlando, A.; Pecile, C. *J. Chem. Phys.* **1979**, *71*, 2282.

(16) Meneghetti, M.; Bozio, R.; Zanon, I.; Pecile, C.; Ricotta, C.; Zanetti, M. *J. Chem. Phys.* **1980,** *80*, 6210.

(17) Kozlov, M. E.; Yurchenko, A. A.; Pokhodnia, K. I. *Spectrochim. Acta* **1989**, *45a*, 437.

(18) Kaplunov, M. G.; Lubovskaya, R. N. *Solid State Phys. (Russian)* **1980**, *22*, 3362.

(19) Seeger, D. M.; Korzenietski, C.; Kowalchik, W. *J. Phys. Chem.* **1991**, *95*, 68.

(20) Bozio, R.; Pecile, C. *The Physics and Chemistry of Low Dimensional Solids*; Alcacer, L., Ed.; Reidel: Dordrecht, 1980; pp 165−186.

(21) Rice, M. J.; Lipary, N. O.; Strassler, S. *Phys. Rev. Lett.* **1977**, *39*, 1359.

(22) Lipary, N. O.; Rice, M. J.; Duke, C. B.; Bozio, R.; Girlando, A.; Pecile, C. *Int. J. Quantum Chem. Symp.* **1977**, *11*, 583; **1978**, *12*, 545(E).

(23) Pokhodnia, K. I. *Acta Phys. Pol.* **1995**, *87*, 815.

(24) Cavara, L.; Gerson, F.; Cowan, D.; Lerstrup, K. *Helv. Chem. Acta* **1986**, *69*, 141.